Hindawi
International Journal of Aerospace Engineering
Volume 2023, Article ID 9378776, 15 pages
https://doi.org/10.1155/2023/9378776

Research Article

The Influence of Bleeding Direction on Starting Performance of Three-Dimensional Inward Turning Inlet

Tianyu Gong,[1] **Yiqing Li**,[1] **Feng Wei**,[2,3] **Shiqichang Wu**,[1] **and Dehua Cao**[1]

[1]*School of Aircraft Engineering, Nanchang Hangkong University, No. 696, Fenghenan Road, Nanchang, 100190 Jiangxi, China*
[2]*Science and Technology on Scramjet Laboratory, China Aerodynamics Research and Development Center, No. 6, Second Ring Road, Mianyang, 621000 Sichuan, China*
[3]*Aerospace Technology Institute, China Aerodynamics Research and Development Center, No. 6, Second Ring Road, Mianyang, 621000 Sichuan, China*

Correspondence should be addressed to Yiqing Li; yiqingli@nchu.edu.cn

Received 29 November 2022; Revised 29 May 2023; Accepted 17 July 2023; Published 29 August 2023

Academic Editor: Kan Xie

Bleeding is an effective method to improve the starting performance of the inlet, and the conventional method often adopts the bleeding to longitudinal direction. This article proposes the use of transversal bleeding method to explore the influence on starting capacity by changing the bleeding direction. The paper designs 6 bleeding inlets. By calculating the starting performance, it is found that the projected bleeding rate of the inlet, which is the direct factor influencing the starting performance, would change due to the direction change of bleeding, although designed with the same entrance. For the inlet designed with longitudinal slots and bleeding, it could reach the starting state at Mach 3.6, but it showed the unstart state when they are transversal direction. The same entrance, when inlet is designed by transversal bleeding with longitudinal slots, the starting Mach number would decrease to 3.8. For the changes of aerodynamic capabilities, there would be the "point jump" tendency when reaching starting state, but the same inlets would keep the similar performance when they get the starting state.

1. Introduction

Hypersonic aircraft technology has become the research hotspot, which is deeply discussed for the development of aspired hypersonic aircraft [1]. Inlet plays a significant role in the propulsion system of hypersonic aircrafts, majoring in providing the precompressed airflow for the combustion chamber. Therefore, the exploring and designing of inlet are largely puzzled by lower Mach number starting problems, which can restrict the overall performance of the aspired propulsion system. When the inlet unstarts, the precompressed airflow cannot completely enter the combustion chamber, which leads to the fact that the propulsion system cannot normally run [2–5]. The factor separation of boundary layer which exists by the accumulation of lower-energy airflow highly affects the starting capacity of the inlet. In addition, the interference between shock waves and boundary layer is the leading reason restricting the overall performance of aspired hypersonic aircrafts, causing the separation in inlet, making the internal flow field more complex, and reducing the starting capacity of the inlet [6–9].

More recent attention has focused on the provision of improving the starting capacity of the inlet, while most of the researches on improving the starting capacity have been carried out in bleeding or adaptive slots. Bleeding is used to convey the lower-energy airflow relying on the pressure distribution from internal flow field to the outside. Schulte et al. [10, 11] revealed by experiments and numerical simulations that bleeding used in the inlet could reduce the mass flow rate of lower energy with the flow separation decreased and internal flow field quality improved. In addition, bleeding design layout was one of the factors affecting the starting capacity of the inlet. Häberle and Gülhan [12] showed that reasonable bleeding layout helped to appease the interference between shock waves and boundary layer, avoiding the separation of airflow. Fukuda et al. [13] and Mitani et al. [14] demonstrated by experiments that the best position to design the bleeding was located in front of the

isolator near the internal shock wave on the upper surface of the inlet. A function was simulated by changing the bleeding angle for controlling the lower-energy airflow in the inlet, and it showed that the superior designing of bleeding was when it was perpendicular to the flow direction [15]. The researches of Fujimoto et al. [16] and Weixing et al. [17] successfully improved the starting capacity for the bleeding designed at the compression section in the inlet and the interference between shock waves and boundary layer was effectively reduced. In addition, expanding the entrance of bleeding could effectively increase the starting capacity of the inlet. Yuan et al. [18] implemented a way to improve the starting capacity by rising the entrance opening ratio of bleeding. Li et al. [19] presented the loss of mass flow rate when bleeding inlet was considered as the method to perform controlling of the boundary layer to improve the inlet starting capacity. Due to the loss of air flow, Jianyong et al. [20] developed a way of designing an adaptive slot in the inlet wall to avoid the loss of airflow with starting capacity of inlet improved. This method is aimed at guiding the lower-energy airflow to cross through the adaptive slot for the distribution of pressure before and after the shock waves generated by unstarting inlet, and inject into the compression wedge surface of the same level of the inlet wall again, so as to reduce the separation bump on the inlet until it disappears, forming a closed airflow cycle. Zhu et al. [21] investigated the adaptive slot control method to improve the starting capacity of hypersonic inlet, and indicated that the adaptive slot was needed to be arranged based on the position of separation bump. These studies aim at improving the starting capacity of inlet and solve the problem of airflow loss. It is important to mention that the longitudinal bleeding method is widely used in inlet as the boundary layer controlling method, and it may lead to the interference of the forebody in chin layout. Therefore, it is necessary for the three-dimensional inward turning inlet to perform the studies on the characteristics of boundary layer controlling with different directions of bleeding.

Based on these studies, this paper focuses on the analysis of the influence of different bleeding ways on the inlet starting capacity by changing the direction of bleeding, and the results are in contrast with the conventional method. In addition, all the inlet bleedings are arranged perpendicular to the airflow direction. This study is expected to affecting the starting capacity of the inlet with the inlet designed by different direction of bleeding.

2. Physical Models and Numerical Method

Three-dimensional inward-turning inlet is widely used in the design and development of hypersonic aircrafts. The major advantages of this inlet are the higher compression efficiency and stronger airflow capture ability [22–24]. Therefore, different direction bleeding designed in inlets are considered as the studying objects in this paper in order to study the influence of the starting capacity generated by bleeding direction. The basic inlet is developed by streamlines tracing at Mach 6 and height 26 km. According to the bleeding direction, the bleeding designing considers two methods so as to study the effect of the starting capacity presented by the bleeding direction. The first one is that the bleeding is generated by the entrance lines with transversally or longitudinally extending. The second one is that array bleeding slots are designed as the beginning of bleeding with extending bleeding as the end. All the bleedings are introduced at the upper compression surface. Figure 1 shows the original basic inlet and different bleeding directions inlet models with an internal compression ratio of CR = 4.5534.

All these inlets are simulated by Fluent with the SST k-ω turbulence model, while treating the phenomenon that airflow in the throat of inlet can work normally as the judgement standard of starting. The SST k-ω turbulence model mainly considers the transport of turbulent shear stress, which could limit the vortex viscosity in rapidly deformed flows and better predict strong reverse pressure gradients and separated flows. And the specific forms of the turbulent kinetic energy transport equation and the turbulent specific dissipation rate equation could be regarded as follows:

$$\frac{\partial \rho k}{\partial t} + \frac{\partial \rho u_j k}{\partial x_j} = \frac{P_k}{\mathrm{Re}_\infty} - \beta^* \rho k\omega + \frac{1}{\mathrm{Re}_\infty}\frac{\partial}{\partial x_j}\left[(\mu_L + \sigma_k \mu_T)\frac{\partial k}{\partial x_j}\right],$$

$$\frac{\partial \rho \omega}{\partial t} + \frac{\partial \rho u_j \omega}{\partial x_j} = \frac{\gamma \rho P_\omega}{\mathrm{Re}\ \mu_T} - \beta \rho \omega^2 + \frac{1}{\mathrm{Re}_\infty}\frac{\partial}{\partial x_j}\left[(\mu_L + \sigma_\omega \mu_T)\frac{\partial \omega}{\partial x_j}\right] + 2\rho\frac{(1-F_1)\sigma_{\omega 2}}{\mathrm{Re}_\infty \omega}\frac{\partial k}{\partial x_j}\frac{\partial \omega}{\partial x_j}. \quad (1)$$

3. Results of Bleeding with Same Section

3.1. Mesh Validation. Mesh validation in this paper is verified through the calculating the aerodynamic coefficients of hypersonic aerospace plane and the pressure distribution of the inlet wall. The hypersonic aerospace plane model is shown in Figure 2. The mesh of aerospace airplane in Figure 3 was divided by polyhedral mesh, trim mesh, and tetrahedral mesh. Table 1 shows the lift coefficient and the error change contrasted with the experimental results by different mesh number, and Figure 4 loads the scatter diagrams of aerodynamic coefficient change in different attack of angles. Totally, the lift coefficient calculated by different numbers of mesh is accurate with the experimental result by the contract of error change. Besides, the lift and drag coefficients calculated in little attack of angles are similar with the experimental results. Therefore, the shock wave flow field contours in Figure 5 simulated by different mesh types could be extremely coincident with experimental consequence at attack of angle of 0° on the structure of shock wave. Above all, using these kinds of meshes could present the hypersonic results and the shock wave flow field accurately.

For the result in this table, CL and CD are the characters of hypersonic aerospace airplane lift and drag coefficients, while CL* is the character of error between lift coefficient by simulation methods and experimental result. Besides,

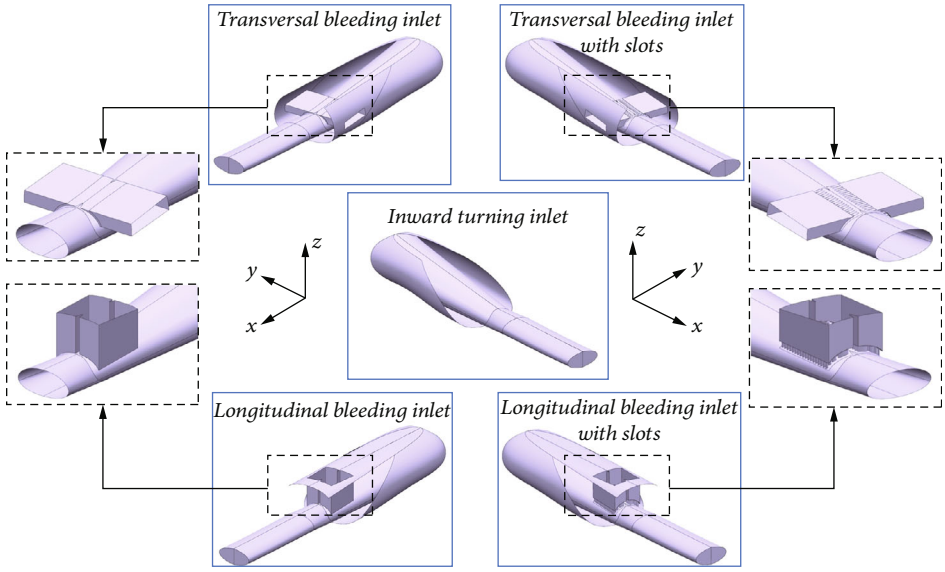

Figure 1: Bleeding inlet models in different methods.

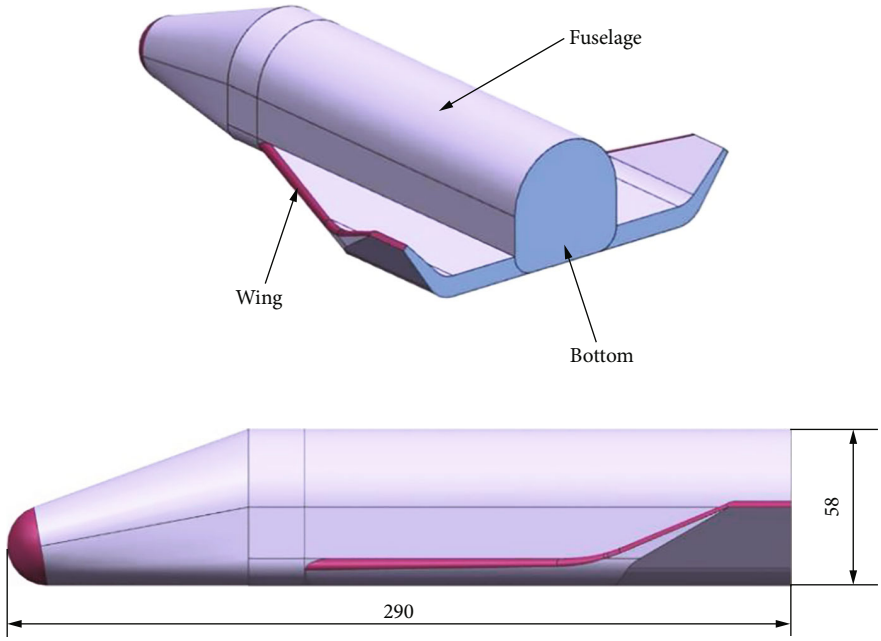

Figure 2: Hypersonic aerospace plane model.

the calculating results and the experimental results are referred to references [25].

The calculation condition starts with Mach 3. When the inlet unstarts, the coming airflow Mach number is increased until the inlet reaches starting, while the Mach number variation tolerance range is 0.1~0.2. Due to the symmetrical characteristics of the inlet and to the fact that there is no need to consider the condition of sideslip, the calculation process is simulated with half-model structure. Figure 6 shows the structural mesh of inlet with transversal bleeding. Structural mesh is used by inlets without array bleeding slots to calculate, and the trim mesh way is carried on the other inlets. The phenomenon is considered as the convergence standard when all the aerodynamic parameters include the mass flow rate, total pressure recovery coefficient, and Mach number of the outlet keep relative stability. In order to obtain the shock wave structure and calculation results of the airflow field more accurately, the mesh in the internal part of the inlet channel is locally densified.

At the basement of the calculating a dynamic coefficients by hypersonic aerospace airplane, the validation analysis is calculated with the transversal bleeding inlet model at different mesh numbers from 3.0 to 4.5, in order to determine the mesh validation. In addition, the final results indicated the pressure distribution of the inlet surface and the aerodynamic results of the outlet. A similar trend of pressure

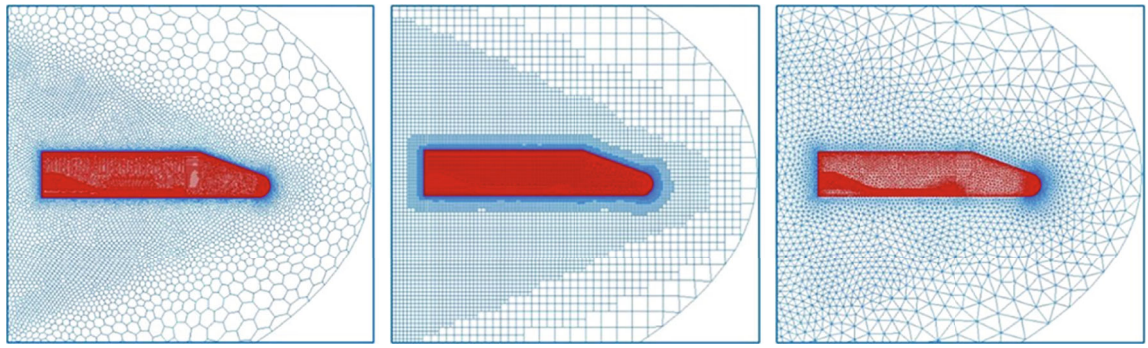

Figure 3: Different mesh divide of hypersonic aerospace plane.

Table 1: Mesh validation results of hypersonic aerospace airplane.

Mesh type	Mesh number	CL	CL*
Coarse mesh	2.49 million	-6.0708*E*-02	4.3184*E*-03
Medium mesh	4.27 million	-6.1041*E*-02	6.1150*E*-03
Fine mesh	6.48 million	-6.0979*E*-02	5.0931*E*-03

distribution as that in Figure 7 can be detected with inlet in different mesh numbers. Due to the increase of the distance of X, the coincidence degree is gradually reduced. Thus, the mesh dividing method and the numbers of the mesh are appropriate to simulate the far field of inlet. Moreover, it is decent to calculate the starting capacity and the aerodynamic performance of bleeding inlet using this method. According to different mesh numbers, the inlet model is divided into coarse mesh (number 2 million), medium mesh (number 3.5 million), and fine mesh (number 4.5 million). For the simulations, pressure-far-field boundary is chosen on the incoming, and the exits of flow field and inlet select the boundary of pressure outlet. Besides, all the walls are considered as wall without slipping, and the symmetry boundary is used in symmetrical plane.

Less error values of aerodynamic parameters in different densities of mesh can be realized through the calculation results simulated by the transversal bleeding inlet, as shown in Table 2. All the error values are calculated with the comparison of fine mesh results. Due to the less error values of aerodynamic parameters at the outlet of the inlet, the mesh validation of the numerical simulation of the model is verified. It shows that the divided mesh has sufficient accuracy to analyze the starting capacity and aerodynamic performance of the bleeding inlet.

3.2. Starting Capacity Analysis of Bleeding with Same Section. In this section, a series of simulations are performed at different Mach numbers ranging from 3.0 to 4.5 of the basic inlet without bleeding. Due to the higher content of lower-energy airflow near the entrance and the wall of the inlet when in the case of Mach 4.5, the internal space is filled with boundary layer on the upper surface of the inlet, while the separation is generated for the interference by the shock waves inside. In addition, the outlet is nearly occupied by lower-energy airflow with the serious loss of total pressure recovery coefficient, which is less than 0.36, as shown in Figure 8. Thus, abnormally running is resulted in the airflow jam at the throat of the inlet, and it is hard for the chosen inlet model to realize starting, while the bleeding method is devised to improve the starting capability in this paper.

In order to achieve the ability that the designing of bleeding can improve the starting capacity of the inlet, bleeding is arranged at the internal compression section of the inlet. The inlet model with bleeding is shown in Figure 1, and the difference is determined on the direction of bleeding, while the same area is selected as the bleeding entrance. Due to the direction change, the projection bleeding entrance presents different area. Therefore, the projection bleeding rate (R_{PB}) would be changed when the direction changes, which is defined as the ratio of the area of projection bleeding entrance and the actual inlet entrance area. For the two inlets, the projection bleeding rate of the Y -direction bleeding inlet is 0.2003, and the projection bleeding rate of the Z-direction bleeding inlet is 0.4623.

After that, several simulations are performed to verify the effect on improving the starting capacity. The Mach contours of inlet are shown in Figure 9, where an improvement of the basic inlet model on the starting capacity can be shown due to the arrangement of transversal bleeding at the inlet surface. With the increase of the inflow Mach number, the lower-energy airflow is gradually reduced at the throat of the inlet through the transversal bleeding, and the structure of shock waves in the far field of inlet becomes accurate when Mach is equal to 3.5.

Compared with the results calculated by transversal bleeding inlet, the interference generated at the throat of the inlet is much severe when the longitudinal bleeding method is performed in the inlet. When the longitudinal bleeding is arranged in the inlet to improve the starting capability, the airflow from the exit of the bleeding would affect the field on the upper surface of cowl. In addition, the most sever interaction exists near the bleeding entrance, in which shock waves in the inlet are more easily delivered inside of the bleeding, leading to the interference at the throat of the inlet. Besides, the interference after the entrance of bleeding is clearly shown in Figure 10, and the thickness of boundary layer is larger than the results calculated by transversal bleeding inlet. Therefore, the longitudinal bleeding inlet can cause the phenomenon of worse of the field quality, while the alone similar part is the starting capacity, and it could get the start state at Mach 3.5.

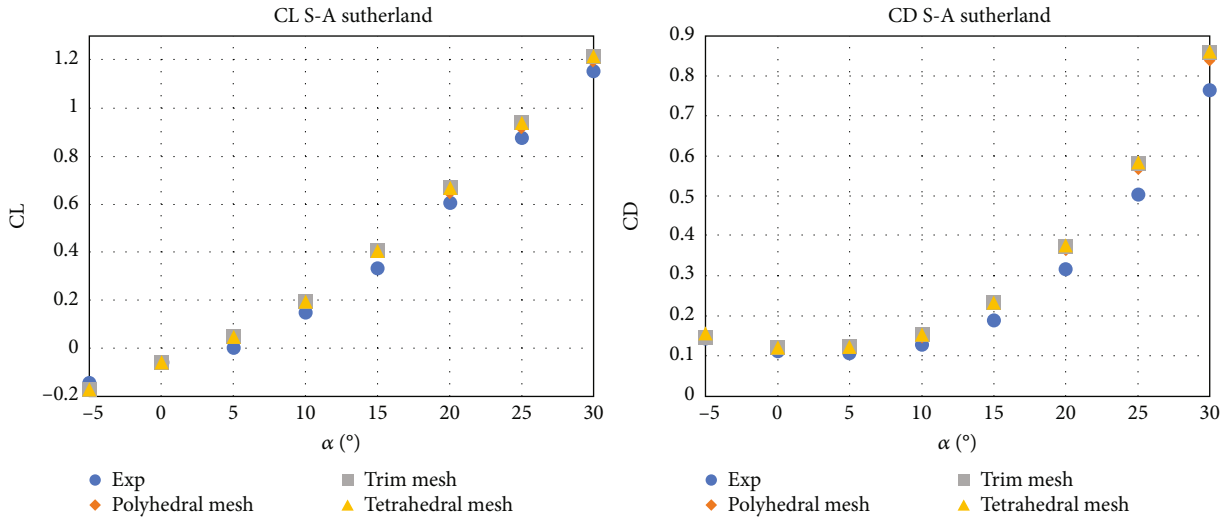

Figure 4: Lift and drag coefficients change by attack of angle increasing.

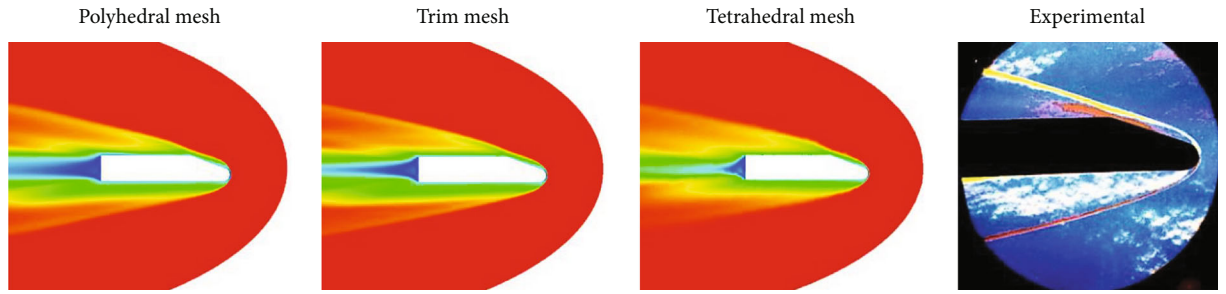

Figure 5: Mach number contours and experimental result at attack of angle 0°.

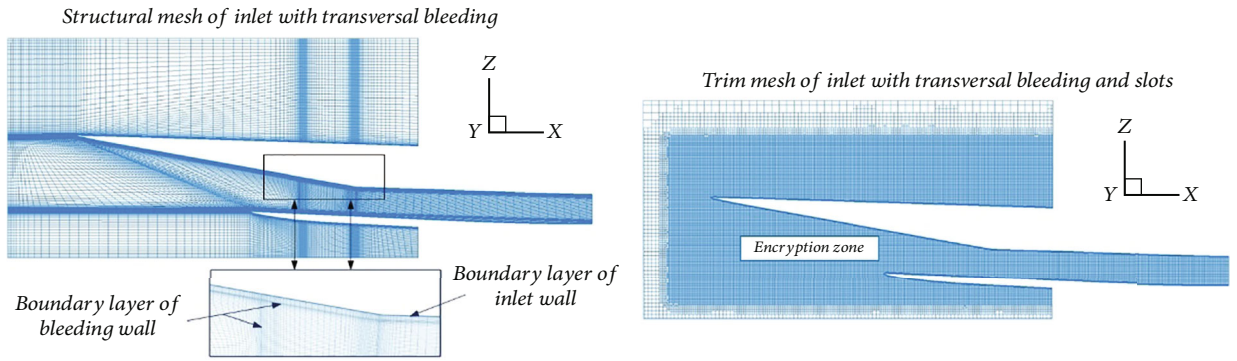

Figure 6: Mesh models of transversal bleeding inlet.

The thickness of lower-energy airflow on the isolator wall is reduced effectively due to the increase of the inflow speed. However, a serious problem exists at the throat of the inlet, in which lower-energy airflow in bleeding easily interacts with shock waves. Therefore, when the Z-direction bleeding is carried on chin layout integration design, there would be an effect occurred by the bleeding air, which would cause the total kinetic energy of inflow decreased.

The pressure distribution of the internal field is calculated, and the line tendency at Mach 3.5 is also illustrated in Figure 11. No error changes are shown in the beginning, but when the distance is larger than 2.3. By comparing the pressure distribution of two bleeding inlets, the longitudinal bleeding way can cause the higher interference with the greater pressure ratio wave and larger range of pressure change at $X = 2.4$. Therefore, the inlet which is carried on transversal bleeding method can improve the starting capability capacity while decreasing the interference. According to these results above, transversal bleeding inlet can make the flow field stable while decreasing the interference and increasing the quality in transversal inlet.

As shown in Figure 12, it is hard to avoid the loss of outlet total pressure recovery coefficient due to the function of bleeding. The results show that the increasing of the inflow

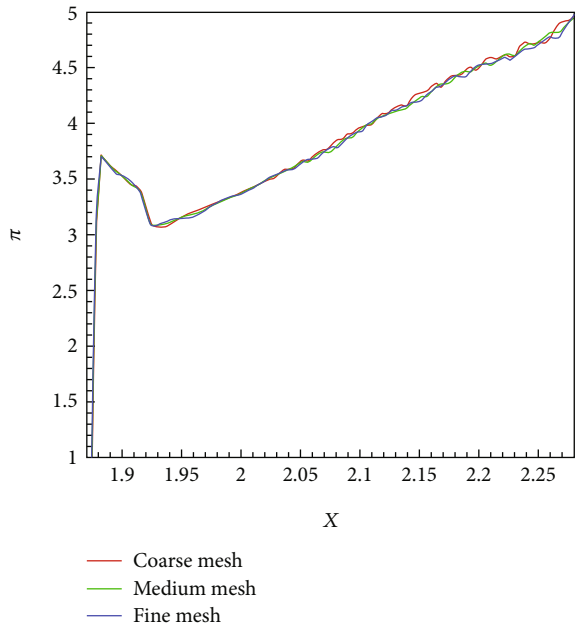

Figure 7: Pressure distribution of the inlet wall.

Mach number could can make the range of outlet total pressure recovery coefficient larger. Compared with the results simulated by the bleeding methods in different directions, the transversal bleeding method inlet leaves results in less loss of total pressure and the higher-pressure distribution area is much wider, whose shape looks like the character "H" character and the maximum value of total pressure recovery coefficient at the outlet is 0.82. The shape looks like the "U" character of the longitudinal bleeding method inlet, and the lower-energy airflow is distributed at the top and the both sides of outlet. However, there is less error of total pressure recovery coefficient range shown on contours, when carrying on the same inflow velocity.

It can be seen that the flow field quality has been improved, and there is no generated influence on the starting capacity when transversal bleeding inlet is chosen to perform the removal of lower-energy in the inlet. Due to the use of transversal bleeding, the interference between shock waves and lower-energy airflow is effectively inhibited. Besides, the energy loss could be decreased at the top and besides of the outlet when transversal bleeding is carried in the inlet. While the influence on the aerodynamic capability of inlet by the change of entrance projection bleeding rate would be demonstrated.

3.3. Aerodynamic Performance Analysis of Bleeding with Same Section. Due to the different bleeding directions, the projection area of entrance shows different size but the actual geometry. The projection bleeding rate is positively correlated with the projected area of bleeding entrance and exit along the extending direction of bleeding.

A declining tendency is shown for the outlet total pressure recovery coefficient. Transversal bleeding uses the projection bleeding rate of 0.2003, while longitudinal bleeding is 0.4623. Table 3 presents the calculating aerodynamic results

Table 2: Aerodynamic parameters and error of different density meshes.

	Fine mesh	Medium mesh	Coarse mesh
Q	0.92	0.92	0.92
ΔQ	——	0%	0%
$\boldsymbol{\sigma}$	0.52	0.53	0.52
$\boldsymbol{\Delta\sigma}$	——	1.92%	0%
Ma	2.03	2.04	2.03
ΔMa	——	0.49%	0%

(the Mach number, total pressure recovery coefficient, and the mass flow rate).

Figure 13 shows the tendency of aerodynamic parameters of bleeding inlet in different directions with the same section. Larger projection bleeding rate gives expression to the higher mass flow rate of lower-energy airflow in inlet. By increasing the inflow Mach number, all the aerodynamic parameters at the outlet are improved, but the aerodynamic parameters calculated in inlet which are arranged through transversal bleeding would be higher than the one with longitudinal bleeding. Thus, changing the direction of bleeding would make the aerodynamic performance improved, but the starting capability seems stable.

Combining the results in Table 3 and Figure 13, the Mach numbers of the outlet are equal (1.19) when the inflow Mach number is 3.2, while the transversal bleeding inlet could get the mass flow rate and the total pressure recovery coefficient better. The outlet total pressure recovery coefficient calculated by transversal bleeding inlet is 16.1% higher than the one with longitudinal bleeding, and the mass flow rate is increased by 14.3%.

Figure 13 shows the tendency of aerodynamic parameters of bleeding inlet in different directions with the same section. By increasing the inflow Mach number, all the aerodynamic parameters at the outlet are improved, while increasing the range of parameters at the outlet of the transversal bleeding inlet is higher. When the inlet Mach number is 3.2, the outlet Mach numbers of the two inlet models are equal (1.19), the total pressure recovery coefficient is increased by 16.1%, and the mass flow rate is increased by 14.3%. For the state of Mach 3.6, both of the inlets realize the starting capability. While the outlet Mach number of inlet models with transversal bleeding would be higher than the longitudinal one at 0.06, besides, the total pressure recovery coefficient is increased by 16.4%, and the mass flow rate is increased by 12.9%. With the case at Mach 4, the outlet Mach numbers, the total pressure recovery coefficient, and the mass flow rate would be increased by 4.2%, 13.7%, and 8.8%, respectively.

Totally, different results would be depicted in the inlet with different directions of bleeding, but the bleeding entrance would show the same area. And the main factor is determined by the projection bleeding rate which is relevant to the direction of the bleeding. Therefore, it is clear that increasing the projection bleeding rate can easily cause loss of airflow more serious, while the error would be decreased when the inflow Mach number is higher than starting state.

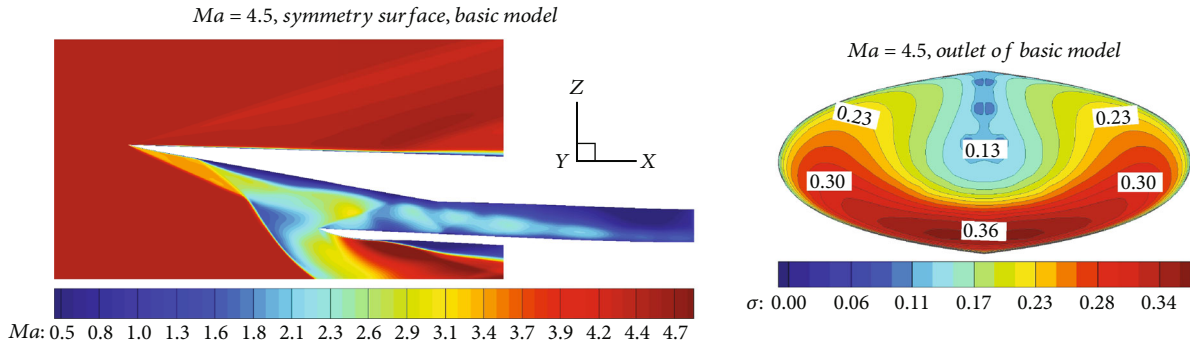

Figure 8: Aerodynamic performance of the basic inlet model.

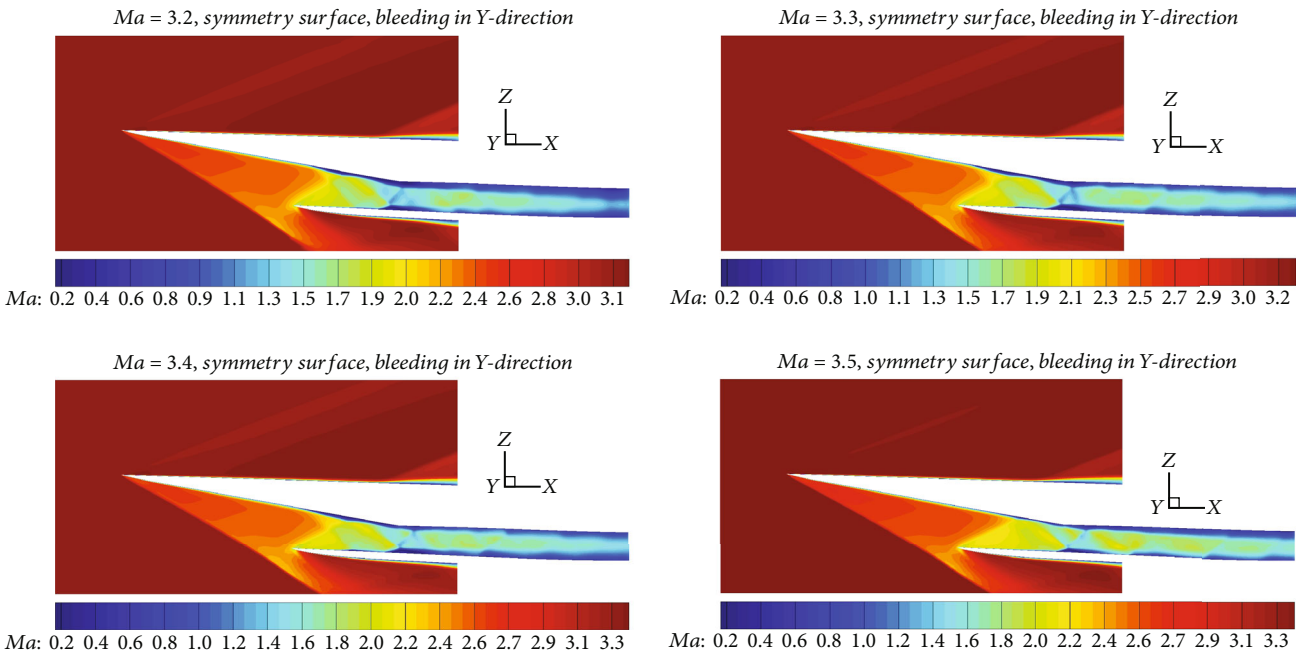

Figure 9: Mach number contours of flow field in transversal bleeding inlet.

4. Results of Bleeding with Array Bleeding Slots

In order to further verify the conclusion that the improvement of starting capability and aerodynamic capability by the change of entrance projection bleeding rate, bleeding with the same direction of slots is arranged in inlet to simulate the function.

4.1. Starting Capacity Analysis of Inlet in Same Bleeding Direction. Figure 14 shows the symmetrical surface Mach number contours distribution of inlets carried on the same bleeding direction. For the conditions of these simulations, only the inlet which is devised with longitudinal bleeding and slots could get the starting state, and the state is at Mach 3.6. However, the transversal bleeding inlet fails to reach the starting condition. Thus, the results show the different conclusions with the cases above. Although the same hole is selected as the entrance of bleeding or slots, there is a factor, projection bleeding rate, changed by changing the bleeding direction to influent the starting performance. By the analysis of the Mach number contours, outflowing would be seriously existed when the slots and bleeding are projected towards the transversal direction, and it could not reach the starting state even in Mach 4.0. On the contrary, when the slots and the bleeding are devised towards to the top direction, the inlet would delay the starting state until Mach 3.6.

Compared with the results without slots, the starting performance has decreased because of the declining of the projection bleeding rate. Therefore, inlet designed with slots could reduce the interference created by the internal shock waves and the lower-energy airflow. It is deduced that longitudinal slots and bleeding has the better quality at the throat of inlet with the mass of lower-energy airflow on the isolator wall reduced. Up to the cowl, due to the lower-energy air outflowing from the inlet, the out environment would be seriously by these lower-energy flow displaced. Thus, there is no improvement when the bleeding direction is longitudinal, while there would be interference when the chin layout is chosen just like the model

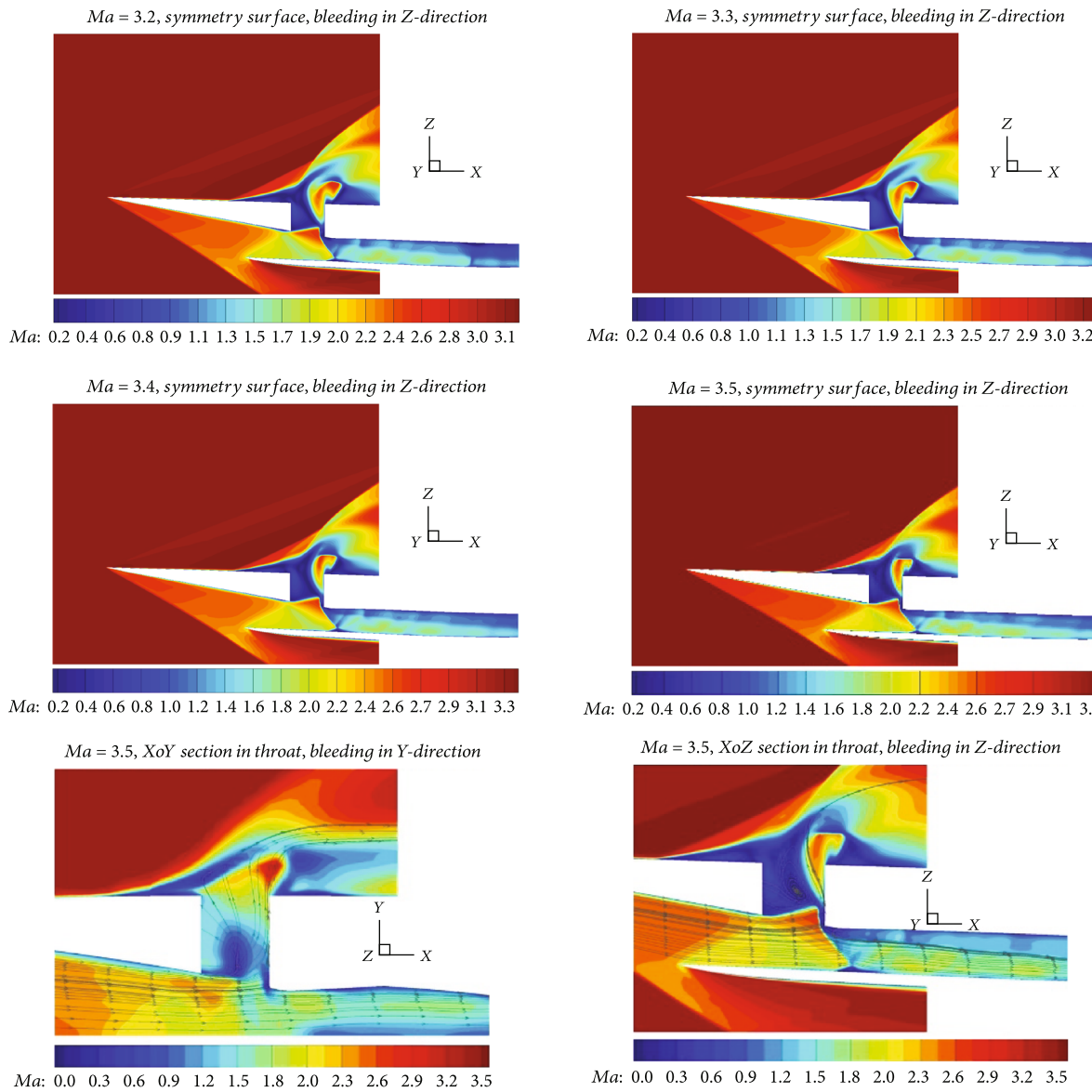

Figure 10: Mach number contours of flow field in longitudinal bleeding inlet.

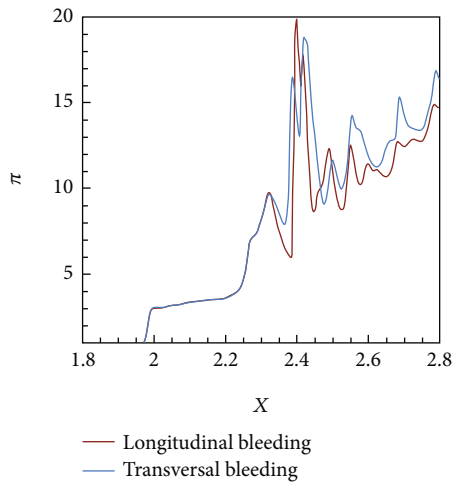

Figure 11: Pressure distribution of the internal field.

whose bleeding is designed towards the longitudinal direction.

Shock wave conveying is clearly shown in Figure 15, which presents the contours of pressure distribution at the symmetrical surface. Amounts of larger pressure airflow exist at the inlet entrance, and separation is easily generated during the unstart states. However, when the inlet passes to the starting capacity, the larger pressure airflow is reduced, and the internal shock waves are normally propagated. By comparing the inlet with and without slots, it can be seen that the same bleeding entrance geometry carried on inlet may lead to different simulating results.

Most importantly, when slots are arranged in inlet to realize the starting capability improved, although the same entrance was arranged in improving the starting capability of inlet, the projection bleeding rate in different direction has changed. For the inlet with longitudinal slots and inlet,

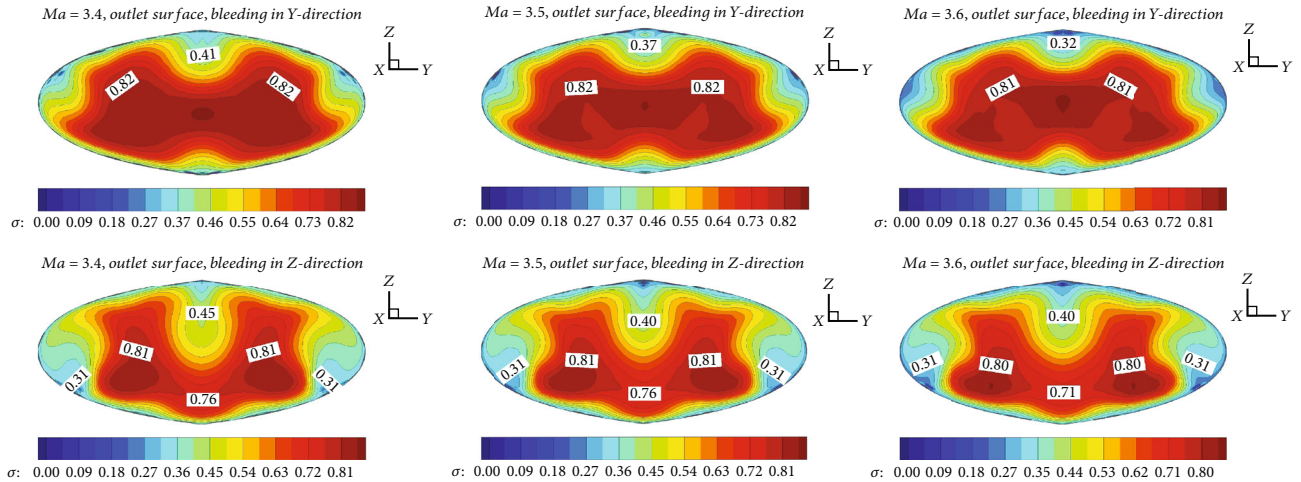

Figure 12: Total pressure recovery coefficient contours of bleeding inlet with the same section.

Table 3: Aerodynamic parameters of bleeding methods without slots.

Ma_{in}	Y-direction bleeding inlet ($R_{PB} = 0.2003$)			Z-direction bleeding inlet ($R_{PB} = 0.4623$)		
	Ma_{out}	σ	Q	Ma_{out}	σ	Q
3.2	1.19	0.72	0.72	1.19	0.62	0.63
3.4	1.32	0.67	0.75	1.28	0.58	0.65
3.5	1.39	0.65	0.77	1.35	0.57	0.68
3.6	1.47	0.64	0.79	1.41	0.55	0.70
3.8	1.60	0.61	0.84	1.54	0.53	0.76
4.0	1.73	0.58	0.87	1.66	0.51	0.80

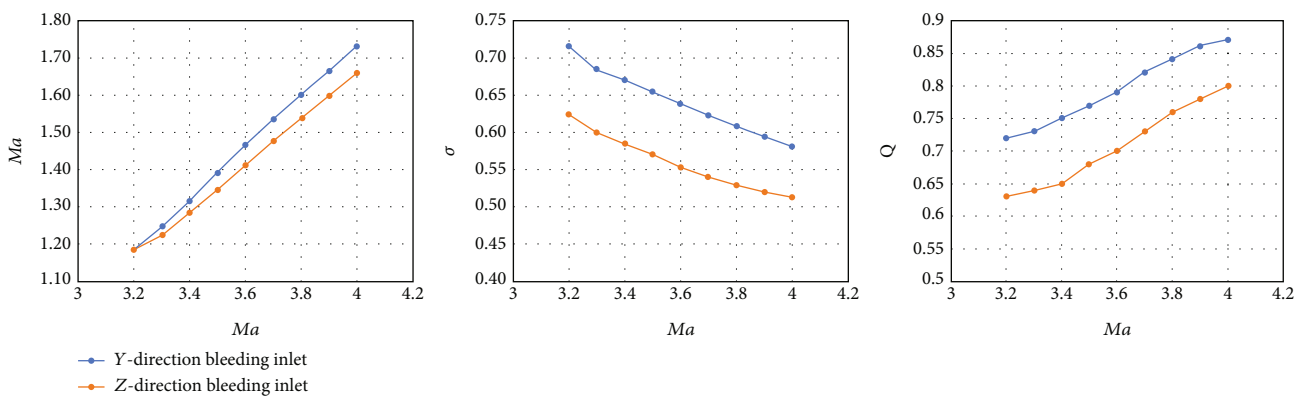

Figure 13: Tendency of aerodynamic parameters of bleeding inlet.

the projection bleeding rate declines to 0.1728, while the projection bleeding rate decreases to 0.0747 when the transversal bleeding and slots are designed in inlet. Owing to the difference of the projection bleeding rate, the inlet would represent the different starting results. For the bleeding inlet with the projection bleeding rate at 0.1728, it could achieve the starting at the state of Mach 3.6. However, inlet with transversal bleeding and slots would not start when the state is Mach 4.0. Thus, the actual factor on affecting the starting state of inlet is the projection bleeding rate. At the same time, it is important to mention that the internal flow field is greatly improved due to the decrease of boundary layer on the isolator wall. In addition, the delivering of shock waves becomes normal at the entrance of slots.

4.2. Starting Capacity Analysis of Inlet in Different Bleeding Directions. When slots and bleeding in the transversal direction method are conducted in the inlet, it is hard to reach the starting capacity, as shown in Figures 14 and 15. This study considers that the bleeding exit may be the reason that makes the inlet unstart, and a new inlet model is designed by widely increasing the size of the bleeding exit. The simulation results are shown in Figure 16. It can be seen that there is no function when the exit of bleeding is widened.

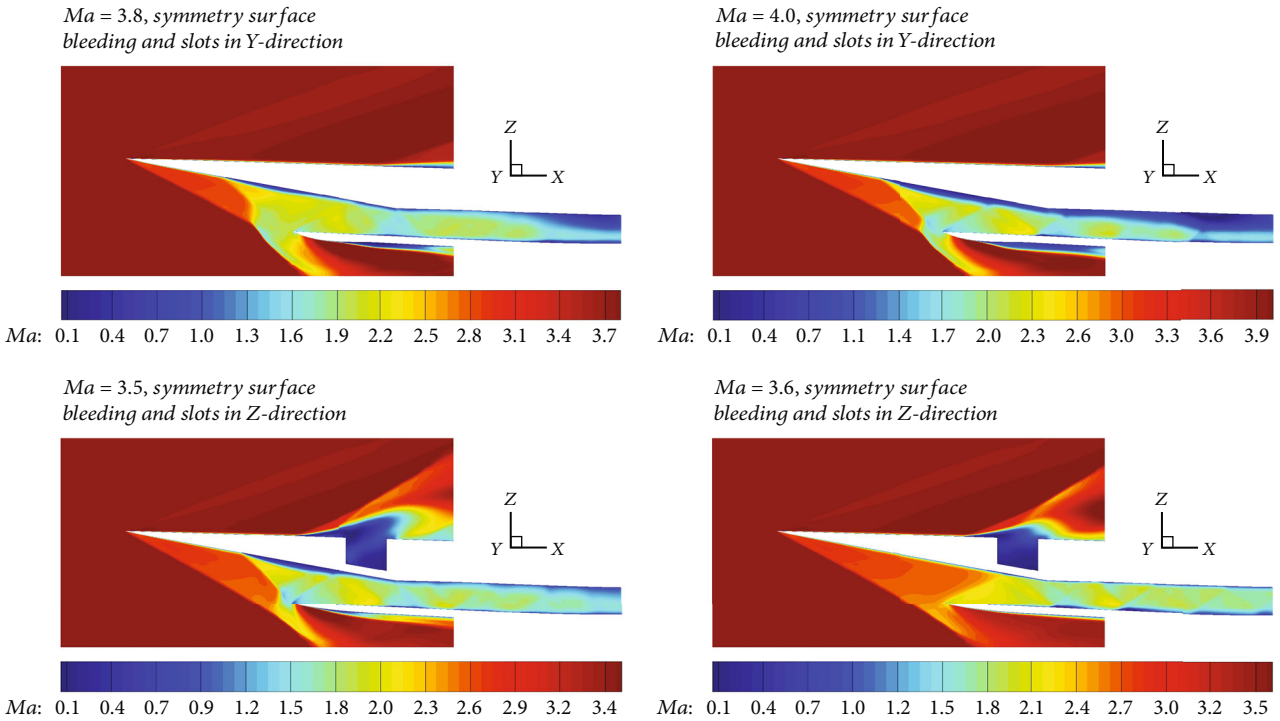

Figure 14: Mach number contours of flow field in bleeding inlet with the same direction slots.

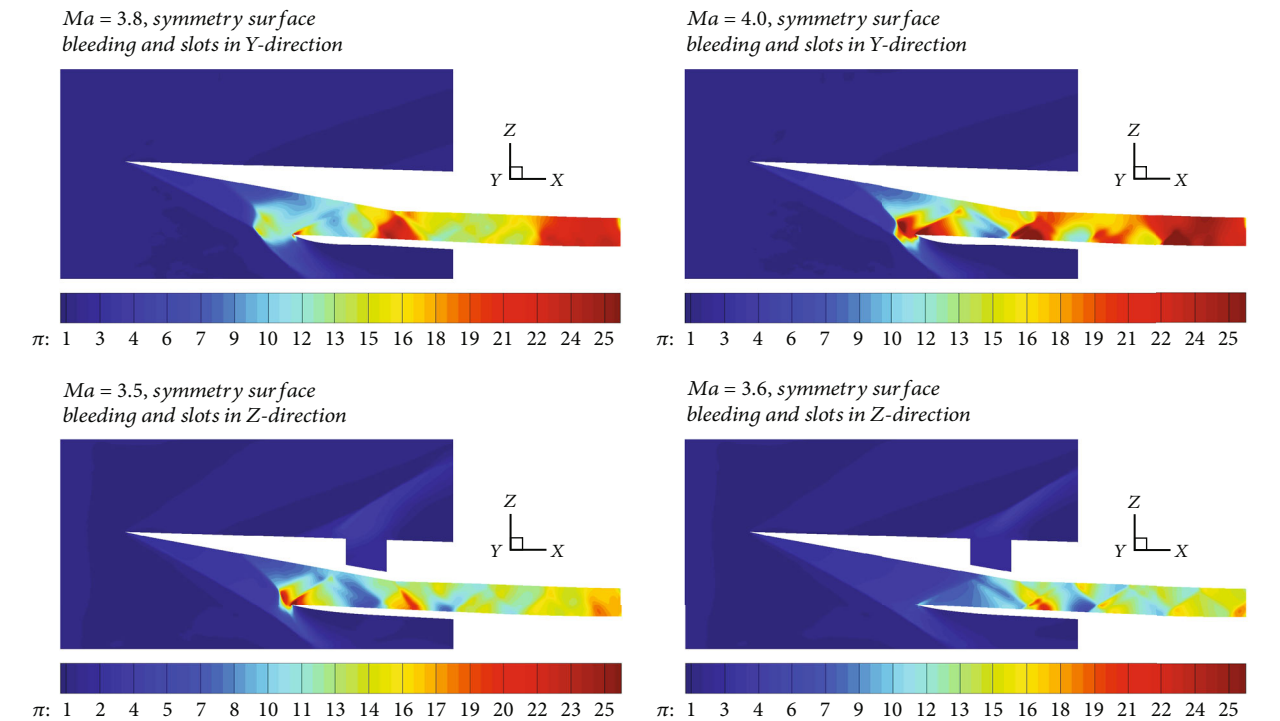

Figure 15: Pressure ratio contours of flow field in bleeding inlet with the same direction slots.

At the same flow speed, boundary layer has no effect at the entrance of slots. On the contrary, a large area of boundary layer is generated on the lower surface of bleeding, which seriously affects the displacement of lower-energy flow. Therefore, the enlarging of bleeding outlet has no impact on improving the starting capacity while making the flowing worse.

Based on the results above, the changing bleeding direction method is carried out to testify the influence on starting performance resulting from the projection bleeding rate. On the one hand, the inlet with transversal slots is arranged with the longitudinal bleeding, and the projection bleeding rate is 0.0747. On the other hand, the other inlet is designed with

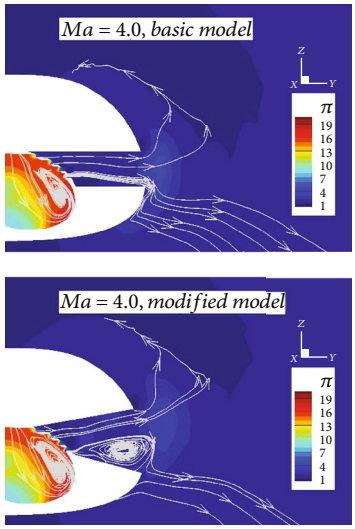

Figure 16: Pressure ratio contours of inlet throat with streamlines.

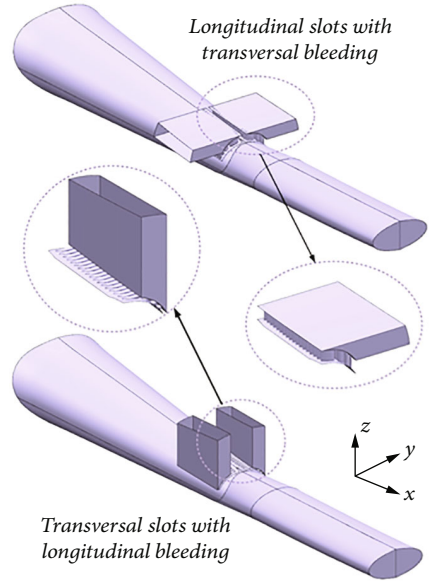

Figure 17: Bleeding inlet with perpendicular direction slots.

transversal bleeding and longitudinal bleeding, while the projection bleeding rate is 0.1728. And the final inlet models with bleeding method are depicted in Figure 17.

The contours on simulating the starting performance of the bleeding inlet are shown in Figure 18, which was arranged with the perpendicular slots. Although the bleeding direction has been changed, there is no impact on the projection bleeding rate due to the unchanged of slot design. Compared with the results of Figures 14 and 15, the starting performance of the inlet designed with transversal bleeding and longitudinal slots is decreased to 3.8, while the starting state seems to have no improvement on the inlet which is arranged with transversal slots and longitudinal bleeding. Thus, the main factor on starting capability of inlet is the projection bleeding rate, and large projection bleeding rate would be benefit on realizing the starting state. However, perpendicular to arrange the slots and the bleeding, it would like to decrease the starting capability even cause the inlet unstart.

The analysis of pressure distribution contours at the throat of the bleeding inlets with slots is shown in Figure 19. The ratio of pressure at the throat is much higher than the starting state result, which means that amounts of lower-energy airflow stay at the place. While an obvious decline tendency on the ratio of pressure could be depicted at the state of Mach 3.8. For the exit of the bleeding, due to the leaving of the lower-energy airflow from the inlet, the ratio of pressure at the bleeding exit is climbing and higher than the one in the far field. The area with higher pressure exists at the sides when the bleeding is designed toward the transversal direction, while the increasing would exist at the top when the bleeding is designed with longitudinal direction. For the fourth picture of Figure 19 Pressure ratio contours of inlet throat with streamlines, due to the perpendicular design method of bleeding and slots, the top wall of bleeding seems to hinder the flowing of the lower-energy airflow, and it might be the significant reason why the starting performance is declining. Therefore, small vortex is appeared on the lower surface of the bleeding, but it seems to have no effect on the outflowing of lower-energy airflow.

4.3. Aerodynamic Performance Analysis of the Inlet in Different Bleeding Directions. The parameters of starting capacity and projection bleeding rate of bleeding inlets are presented in Table 4, where the longitudinal array bleeding slots are treated at the beginning. Due to the difference of projection bleeding rate, longitudinal slot inlet can easily start. For the cases of these starting inlets, the two different bleeding direction inlets have their own starting characteristics, but the aerodynamic parameters after starting are much similar. Nevertheless, the tendency introduces the diverse spots of the starting inlets. A results comparison shows that the starting Mach number of longitudinal slots with the same direction of bleeding would increase to 3.8. However, the outlet aerodynamic performance is similar when both reach the starting state.

By the analysis of Figure 20 and Table 4, changing the direction of bleeding would have a significant effect on its aerodynamic performance. For the inlet with the same direction of bleeding and slots, the aerodynamic parameters of outlet Mach number and mass flow rate would keep the climbing tendency, while the total pressure recovery coefficient would decrease after the inlet reaches the starting performance. Clearly, there is a "point jumping" tendency when the inflow Mach number is 3.6 where the inlet is just starting. All the aerodynamic parameters of the inlet generate the "point jumping" state, which results in significantly increasing all the aerodynamic parameters. However, the bleeding inlet with the same direction of slots maintains the stable growth in other flight conditions. Most importantly, such the same tendency would occur in inlet which is designed with longitudinal slots and transversal bleeding. After the starting state, both of the inlets have similar aerodynamic parameters because of the same projection bleeding

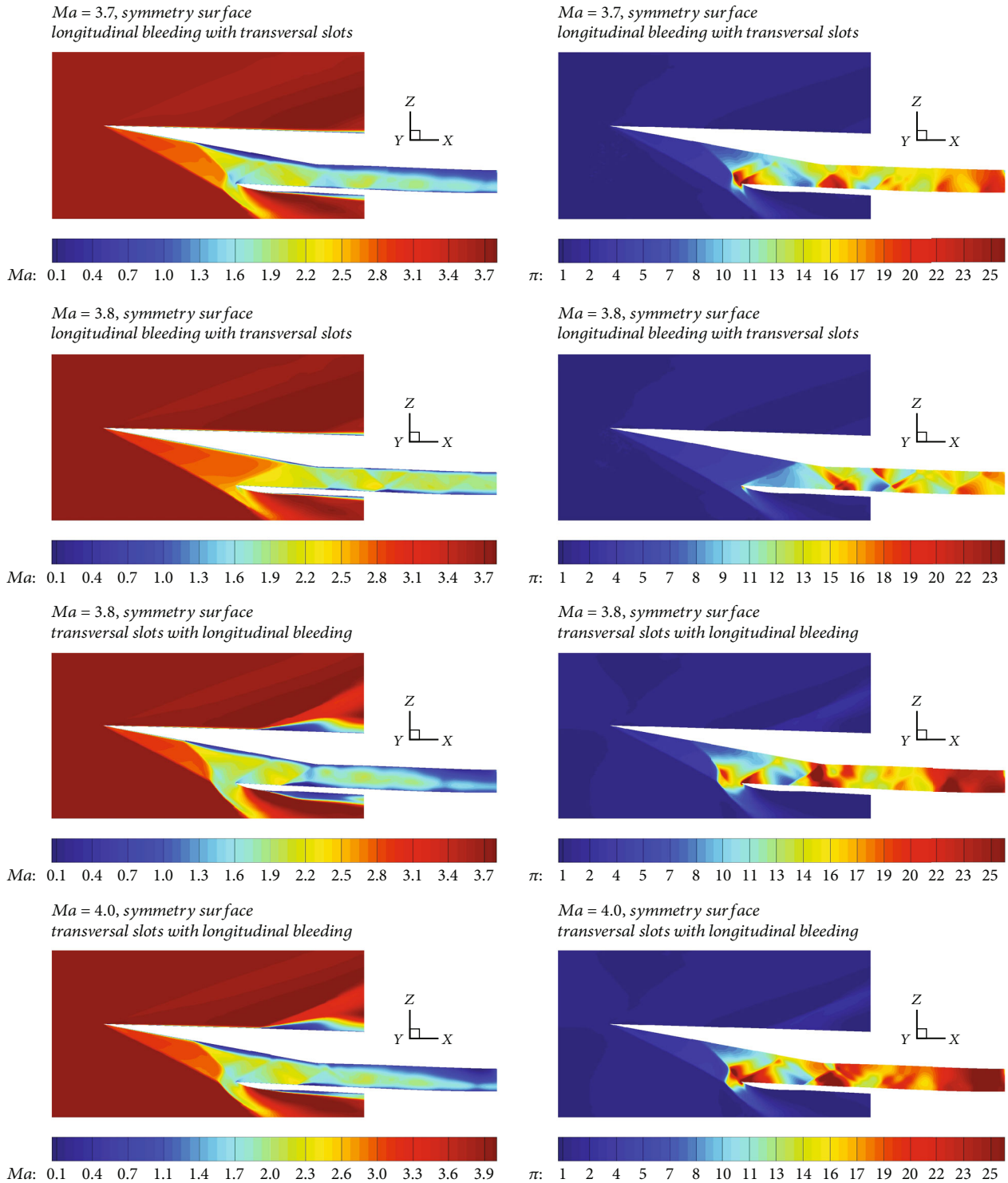

Figure 18: Contours of bleeding inlet with perpendicular direction slots.

rate compared with the results in Figure 13 (tendency of aerodynamic parameters of bleeding inlet).

For the aerodynamic parameters change, there would be three states to introduce. Before the starting performance at the state of Mach 3.5, neither of the inlets achieve starting, and less error is shown in the outlet mass flow rate. However, for the bleeding inlet which uses the same direction of bleeding and slots, the performances of outlet Mach number and total pressure recovery coefficient are 12.4% and 5.4% improved, respectively. When the Mach number is 3.6, the bleeding inlet with the same direction of slots can start. In this state, all the aerodynamic parameters of the inlet generate the "point jumping." Compared with the outlet aerodynamic parameters simulated at Mach 3.5, the

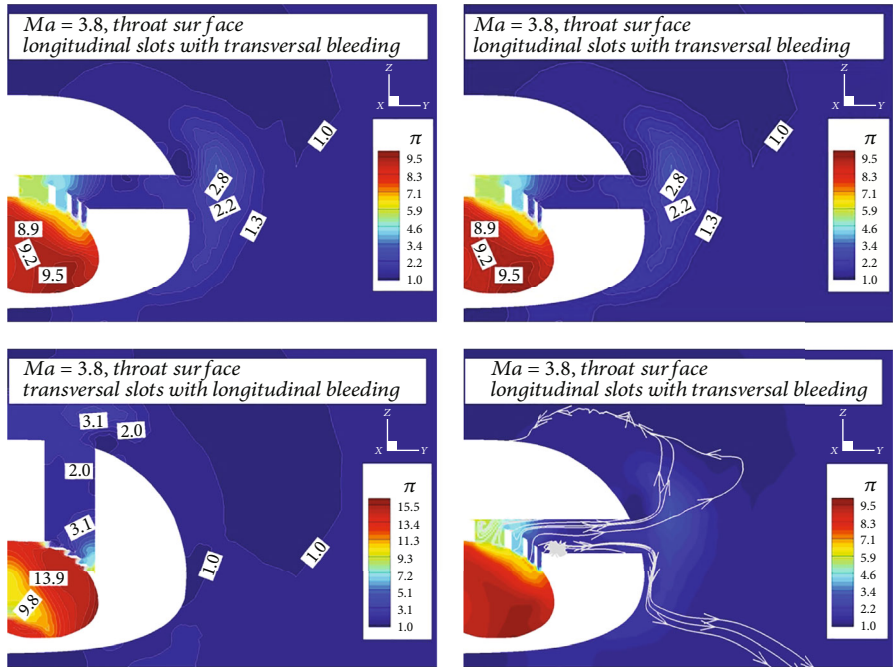

Figure 19: Pressure ratio contours of inlet throat with streamlines.

Table 4: Aerodynamic parameters of different bleeding methods.

Ma_{in}	Bleeding and slots in Y-direction ($R_{PB} = 0.0747$)			Bleeding and slots in Z-direction ($R_{PB} = 0.1728$)			Transversal slots with longitudinal bleeding ($R_{PB} = 0.0747$)			Longitudinal slots with transversal bleeding ($R_{PB} = 0.1728$)		
	Ma_{out}	σ	Q	Ma_{out}	σ	Q	Ma_{out}	σ	Q	Ma_{out}	σ	Q
3.5	Unstart			1.27	0.59	0.76	Unstart			1.13	0.56	0.76
3.6				1.51	0.68	0.84				1.15	0.54	0.79
3.7				1.58	0.67	0.86				1.28	0.53	0.81
3.8				1.65	0.65	0.87				1.63	0.65	0.89
3.9				1.72	0.64	0.88				1.70	0.64	0.90
4.0				1.79	0.63	0.90				1.76	0.63	0.91

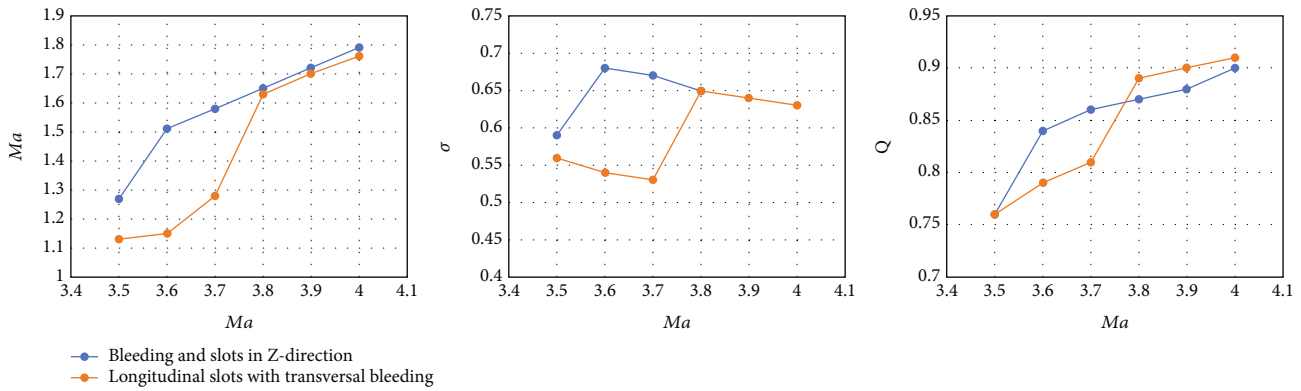

Figure 20: Tendency of aerodynamic parameters of bleeding inlet with slots.

aerodynamic parameters Mach number, total pressure recovery coefficient, and mass flow rate of bleeding inlet with same direction of bleeding slots are increased by 18.9%, 15.3%, and 12.1%, respectively. The starting state of the bleeding inlet with longitudinal slots is Mach 3.8; the "point jumping" tendency is occurred when it starts. Comparing the state of Mach 3.7, the aerodynamic parameters Mach number, total pressure recovery coefficient, and mass flow rate

Table 5: Error of total pressure recovery coefficient and mass flow rate for the difference of entrance projection bleeding rate.

Ma_{in}	Bleeding and slots in Z-direction ($R_{PB} = 0.1728$)				Y-direction bleeding inlet ($R_{PB} = 0.2003$)				Z-direction bleeding inlet ($R_{PB} = 0.4623$)			
	Q	ΔQ	σ	$\Delta\sigma$	Q	ΔQ	σ	$\Delta\sigma$	Q	ΔQ	σ	$\Delta\sigma$
4.2	0.93	—	0.60	—	0.89	96%	0.55	93%	0.83	90%	0.48	81%
4.5	0.96	—	0.57	—	0.92	96%	0.53	93%	0.87	91%	0.45	80%
4.8	0.97	—	0.54	—	0.93	96%	0.50	92%	0.92	95%	0.44	81%
5.0	0.98	—	0.51	—	0.95	97%	0.47	92%	0.93	95%	0.43	83%
5.5	0.98	—	0.44	—	0.96	98%	0.41	93%	0.95	97%	0.36	80%
6.0	0.99	—	0.39	—	0.96	97%	0.36	92%	0.95	96%	0.29	75%

are increased by 27.3%, 22.6%, and 10.8%, respectively. During the the same Mach number at 3.8, the outlet Mach number of bleeding inlet with the same direction slots is higher at 0.02, but the mass flow rate is 0.02 decreased. While the total pressure recovery coefficient plays the same at 0.65 in this state. After the starting performance inflow Mach number, the total pressure recovery coefficient of the bleeding inlet with the same direction slots is equal with the inlet which is designed with transversal bleeding and longitudinal slots, due to the same projection bleeding rate. The inlet designed with transversal bleeding and longitudinal slots plays the less loss on mass flow rate. Therefore, the direction change of the bleeding and slots may reduce the outflow of air caught. On the contrary, an inlet with the same direction of bleeding and slots could keep the higher Mach number of the outlet. Totally, the error of the aerodynamic parameters is much lower after the inlets start.

The mass flow rate, total pressure recovery coefficient, and their error values objective to bleeding inlet with the same direction of slots are shown in Table 5. Enlarging the inflow Mach number after starting, the mass flow rate of inlet would increase close to 1, especially the inlet with lower projection bleeding rate. Therefore, the error of inlet with huge projection bleeding rate would be higher. For the total pressure recovery coefficient, decrease tendency would be shown with the rising inflow Mach number, while the loss of pressure is much higher due to the expanding of projection bleeding rate like the inlet designed with Z-direction bleeding. The loss of total pressure is 75% when the projection bleeding rate is 0.4623.

5. Conclusion

In this paper, the impacts of changing the direction of the bleeding and the connection way of the array bleeding slots on the starting capacity and aerodynamic performance of the three-dimensional inward-turning inlet are studied. The main contributions of this paper are summarized as follows:

Inlet with transversal bleeding would be benefit on the starting performance of the inlet, and the flow field could be improved for the weakness of interference at the throat. And the energy loss could be reduced.

A direction change of bleeding would change the projection bleeding rate of inlet, although the same size hole is used as its bleeding entrance. For this basic inlet model, transversal bleeding methods could reduce the projection bleeding rate, compared with the one which carried out by the methods of longitudinal bleeding ways. The projection bleeding rate of the Y-direction bleeding inlet is 0.2003, while the Z-direction bleeding inlet is 0.4623. The projection bleeding rate of inlet is 0.1728, which is designed with the longitudinal slots, while slots towards Y-direction would not reach the starting state.

An inlet with a huge projection bleeding rate would be starting much easier than the one that is lower. Both the inlet with the only bleeding could start at 3.5. For the decreasing of projection bleeding rate, the starting capability of inlet with transversal bleeding and slots would reduce at Mach 3.6, while the transversal slots with longitudinal bleeding one would decrease to 3.8. But the inlet could not get the starting capability when the slots are designed towards transversal direction.

The key factor affecting the starting capacity of the inlet is the projection bleeding rate, which is relative to the entrance of the bleeding. For the unstart inlet, enlarging the exit of the bleeding has no impact on its starting performance.

The lower-energy airflow in bleeding is much easier to interfere with shock waves in the inlet, which results in increasing the thickness of the boundary layer in the inlet and making the internal flow field more complex. Through the design of array bleeding slots, interference between the shock waves and the lower-energy airflow can be weakened. In addition, the thickness of the boundary layer in the isolator is reduced, and the internal flow field is greatly improved.

For the starting inlets, larger projection bleeding rate can lead to a severe loss of mass flow rate, but the starting Mach number will be reduced. Both the inlets with bleeding could realize starting state at Mach 3.5. Besides, the mass flow rate of the Y-direction bleeding inlet is larger than the one with the Y-direction bleeding at 0.04. The starting state of the inlet with longitudinal bleeding and slots would be weakened at Mach 3.6, and the inlet with longitudinal slots transversal bleeding would not reach starting state until Mach 3.8, while the two inlets keep the similar mass flow rate at 0.41. But neither of the inlet with transversal slots would not reach starting state. After the starting condition, the loss of the mass flow rate and the total pressure recovery coefficient on the inlet with lower projection bleeding rate were less than the higher projection bleeding rate inlet.

Data Availability

The data used to support the findings of this study are included within the article.

Conflicts of Interest

The authors declare that they have no conflicts of interest.

Acknowledgments

This research was partially funded by the National Natural Science Foundation of China (12002144), Science and Technology Project of Jiangxi Provincial Department of Education (20212BAB211015), Graduate Innovation Special Fund Project (YC2021-058).

References

[1] R. K. Scharnhorst, "An overview of military aircraft supersonic inlet aerodynamics," in *50th Aiaa Aerospace Sciences Meeting Including the New Horizons Forum and Aerospace Exposition*, pp. 1–7, Nashville, Tennessee, 2012.

[2] H. Do, S. Im, M. G. Mungal, and M. A. Cappelli, "The influence of boundary layers on supersonic inlet unstart," in *17th Aiaa International Space Planes and Hypersonic Systems and Technologies Conference*, pp. 1–11, San Francisco, California, 2011.

[3] H. Ogawa, A. L. Grainger, and R. R. Boyce, "Inlet starting of high-contraction axisymmetric scramjets," *Journal of Propulsion and Power*, vol. 26, no. 6, pp. 1247–1258, 2010.

[4] J. L. Wagner, K. B. Yuceil, A. Valdivia, N. T. Clemens, and D. S. Dolling, "Experimental investigation of unstart in an inlet/isolator model in Mach 5 flow," *AIAA Journal*, vol. 47, no. 6, pp. 1528–1542, 2009.

[5] J. Masud and F. Akram, "Effect of passive bleed system on an integrated diverterless supersonic inlet," in *49th AIAA Aerospace Sciences Meeting Including the New Horizons Forum and Aerospace Exposition*, pp. 1–12, Orlando, Florida, 2011.

[6] Y. A. N. G. Jimingy, L. I. Zhufei, Z. H. U. Yujian, Z. H. A. I. Zhigang, L. U. O. Xisheng, and L. U. Xiyun, "Shock wave propagation and interactions," *Advances in Mechanics*, vol. 46, no. 1, pp. 541–587, 2016.

[7] D. V. Gaitonde, "Progress in shock wave/boundary layer interactions," *Progress in Aerospace Sciences*, vol. 72, pp. 80–99, 2015.

[8] H. Babinsky and J. K. Harvey, *Shock Wave-Boundary-Layer Interactions*, vol. 32, Cambridge University Press, 2012.

[9] W. Zhenguo, Z. Yilong, Z. Yuxin, and F. Xiaoqiang, "Prediction of massive separation of unstarted inlet via free-interaction theory," *AIAA Journal*, vol. 53, no. 4, pp. 1108–1112, 2015.

[10] D. Schulte, A. Henckels, and U. Wepler, "Reduzierung stossinduzierter Grenzschichtablosung in Hyperschall-Einlaufen mittels Ausblasen," *Aerospace Science and Technology*, vol. 2, no. 4, pp. 231–239, 1998.

[11] D. Schulte, A. Henckels, and R. Neubacher, "Manipulation of shock/boundary-layer interactions in hypersonic inlets," *Journal of Propulsion and Power*, vol. 17, no. 3, pp. 585–590, 2001.

[12] J. Häberle and A. Gülhan, "Investigation of two-dimensional scramjet inlet flowfield at Mach 7," *Journal of Propulsion and Power*, vol. 24, no. 3, pp. 446–459, 2008.

[13] M. Fukuda, W. Hingst, and E. Reshotko, "Bleed effects on Shocka3oundary-layer interactions in supersonic mixed compression inlets," *Journal of Aircraft*, vol. 14, no. 2, pp. 151–156, 1977.

[14] T. Mitani, N. Sakuranaka, S. Tomioka, and K. Kobayashi, "Boundary-layer control in Mach 4 and Mach 6 scramjet engines," *Journal of Propulsion and Power*, vol. 21, no. 4, pp. 636–641, 2005.

[15] W. J. Chyu, M. J. Rimlinger, and T. I.-R. Shih, "Control of shock-wave/boundary-layer interactions by bleed," *AIAA Journal*, vol. 33, no. 7, pp. 1239–1247, 1995.

[16] A. Fujimoto, N. Niwa, and K. Sawada, "Numerical investigation of supersonic inlet with realistic bleed andbypass systems," *Journal of Propulsion and Power*, vol. 8, no. 4, pp. 857–861, 1992.

[17] W. Weixing, Y. Huacheng, H. Guoping, and L. Dewang, "Impact of suction position on starting of hypersonic inlet," *Journal of Aerospace Power*, vol. 24, no. 4, pp. 918–924, 2009.

[18] Y. Huacheng and L. Dewang, "Effect of suction on starting of hypersonic inlet," *Journal of Propulsion Technology*, vol. 6, pp. 525–528, 2006.

[19] L. Yongzhou, Z. Kunyuan, and Z. Liuhuan, "Effect of bleeding on vortex region and starting performance of hypersonic inward turning inlet," *Journal of Aerospace Power*, vol. 31, no. 7, pp. 1630–1637, 2016.

[20] W. Jianyong, X. Lvrong, Z. Hao, and T. Yulin, "A flow-control conception of improving self-start performance of hypersonic inlet," *Acta Aeronautica Et Astronautica Sinica*, vol. 36, no. 5, pp. 1401–1410, 2015.

[21] C. Zhu, R. Yang, R. Chen, R. Qiu, and Y. You, "Investigation of adaptive slot control method for starting characteristics of hypersonic inlets," *Proceedings of the Institution of Mechanical Engineers*, vol. 233, no. 11, pp. 4261–4271, 2019.

[22] X. Wenzhong and G. Rongwei, "Mixed-compression supersonic inlets based on four air-breathing aircraft configurations," *Journal of Nanjing University of Aeronautics & Astronautics*, vol. 43, no. 1, pp. 13–17, 2011.

[23] A. P. Kothari, C. Tarpley, T. A. McLaughlin, B. S. Babu, and J. W. Livingston, "Hypersonic vehicle design using inward turning flow fields," in *AIAA, ASME, SAE, and ASEE, Joint Propulsion Conference and Exhibit, 32nd*, pp. 1–21, Lake Buena Vista, FL, U.S.A., 2006.

[24] Y. Yancheng, L. Dewang, and H. Guoping, "Investigation of internal waverider-derived hypersonic inlet," *Journal of Propulsion Technology*, vol. 27, no. 3, pp. 252–256, 2006.

[25] D. Feng, *Research of a Novel Airframe/Inlet Integrated Full-Waverider Aerodynamic Design Methodology for Air-Breathing Hypersonic Vehicles*, National University of Defense Technology, 2016.